AGU PUBLICATIONS

Geophysical Research Letters

RESEARCH LETTER
10.1002/2016GL069846

Key Points:
- Bipolar seesaw is not a zero-sum transfer of heat between hemispheres but causes a radiative imbalance of ~0.4 W m-2
- During AMOC disruptions, the energy imbalance accumulates in the middepth Atlantic, and is released during resumption
- Energetic impact of AMOC disruptions may have contributed to Quaternary climate instability

Correspondence to:
E. D. Galbraith,
eric.d.galbraith@gmail.com

Citation:
Galbraith, E. D., T. M. Merlis, and J. B. Palter (2016), Destabilization of glacial climate by the radiative impact of Atlantic Meridional Overturning Circulation disruptions, *Geophys. Res. Lett.*, *43*, 8214–8221, doi:10.1002/2016GL069846.

Received 1 JUN 2016
Accepted 23 JUL 2016
Accepted article online 29 JUL 2016
Published online 13 AUG 2016

Destabilization of glacial climate by the radiative impact of Atlantic Meridional Overturning Circulation disruptions

Eric D. Galbraith[1,2,3], Timothy M. Merlis[4], and Jaime B. Palter[4,5]

[1]ICREA, Barcelona, Spain, [2]Institut de Ciència i Tecnologia Ambientals and Department of Mathematics, Universitat Autonoma de Barcelona, Barcelona, Spain, [3]Earth and Planetary Science, McGill University, Montreal, Quebec, Canada, [4]Atmospheric and Oceanic Science, McGill University, Montreal, Quebec, Canada, [5]Graduate School of Oceanography, University of Rhode Island, Kingston, Rhode Island, USA

Abstract During each of the dramatic global warmings that ended the Pleistocene ice ages, the Atlantic Meridional Overturning Circulation (AMOC) was disrupted. It is not clear whether this was a contributing cause or simply an effect of deglaciation. Here we show that in an ensemble of simulations with a global climate model, AMOC disruption causes a consistent and sustained positive radiative imbalance of ~0.4 W m^{-2}. The imbalance is accommodated by heat accumulation in the ocean interior, representing an overall planetary warming, subsequently released by deep convection in the North Atlantic when the AMOC resumes. The results suggest a means by which AMOC disruptions could have helped to tip the planet out of stable glaciated states. However, the fact that AMOC disruptions occurred during prior Heinrich Stadials without causing deglaciation shows that other factors, such as ice sheet dynamics, or controls on CO_2, were also key for deglaciation.

1. Introduction

The ubiquity of Atlantic Meridional Overturning Circulation (AMOC) disruptions during deglaciations is a fascinating observation [*Barker et al.*, 2011; *McManus et al.*, 1999]. On the one hand, deglacial AMOC disruptions could simply reflect such intense freshwater inputs from collapsing ice sheets that the AMOC was consistently overwhelmed [*Broecker*, 1998]. However, it is also possible that AMOC disruptions played a critical role in tipping the climate out of stable glacial states, allowing deglaciation to occur [*Barker et al.*, 2011; *Cheng et al.*, 2009; *Toggweiler and Lea*, 2010]. During the most recent deglaciation, the interval between ~17.5 and 14.5 ka, known as Heinrich Stadial 1 (HS1) stands out as a critical time when atmospheric CO_2 rose rapidly, the ice sheets began to collapse, and the AMOC was disrupted [*Barker et al.*, 2009; *Broecker*, 1998].

It is possible that deglacial AMOC disruptions contributed to the destabilization of glacial climates by causing an oceanic release of atmospheric CO_2, thereby warming the planet [*Cheng et al.*, 2009]. Models and observations suggest that the behavior of the Southern Ocean was key to the CO_2 release [*Jaccard et al.*, 2016; *Köhler et al.*, 2005], implying that if AMOC disruptions did cause the CO_2 to rise, they did so by triggering the Southern Ocean to release CO_2, as may have occurred via an alteration of the global ocean density structure [*Menviel et al.*, 2014; *Schmittner and Galbraith*, 2008] or a shift of the southern westerly winds [*Anderson et al.*, 2009; *Lee et al.*, 2011]. In addition to CO_2 changes, destabilization could have occurred due to physical impacts of AMOC disruption. Subsurface warming of the North Atlantic Ocean has been shown in models as a direct result of an AMOC disruption [*Alvarez-Solas et al.*, 2011; *Liu et al.*, 2009] and has been well corroborated by observations [*Dokken et al.*, 2013; *Thiagarajan et al.*, 2014]. This local oceanic warming could have melted the base of floating ice shelves, destabilizing the marine-based Laurentide ice sheet [*Alvarez-Solas et al.*, 2010; *Marcott et al.*, 2011] and tugging it toward collapse. Here we highlight and explore an additional destabilization mechanism, which brings further significance to the observed subsurface Atlantic warming: AMOC disruptions would have caused net planetary warming, providing an additional push toward the collapse of the glacial ice sheets.

AMOC disruptions have long been associated with antiphased temperature changes recorded in ice cores from Greenland and Antarctica, known as the "thermal bipolar see-saw" [*Broecker*, 1998]. According to this idea, the northward transport of heat by the Atlantic Meridional Overturning Circulation (AMOC) was periodically disrupted, redirecting low-latitude warmth to the Southern Hemisphere [*Crowley*, 1992] where it

gradually accumulated in the Southern Ocean [*Stocker and Johnsen*, 2003]. The net result would have been a colder Northern Hemisphere, contrasted with a warmer Southern Hemisphere. The traditional view of the bipolar seesaw implicitly considers the Earth surface as a closed system, in which changing the transfer of heat between hemispheres by the ocean circulation warms one at the expense of the other, with no net global heating or cooling.

However, the total heat content of the ocean-atmosphere system is determined by the radiative balance between the absorbed shortwave (ASW) and outgoing longwave radiation (OLR) for the planet, both of which depend on climate state. Prior coupled model simulations have shown that the global planetary radiative balance is sensitive to AMOC shutdowns, both in freshwater-forced simulations [*Drijfhout*, 2015; *Vellinga et al*., 2002] and in the unforced AMOC oscillations of *Peltier and Vettoretti* [2014]. Most of these simulations have been quite short (centuries or less), and the radiative imbalance has been shown to differ substantially between models of varying complexity [*Drijfhout*, 2015], raising questions about their representativeness. In addition, the radiative impact of AMOC shutdowns might be expected to vary significantly as a function of the background climate state, which has not been previously explored. In order to better characterize the radiative impact of AMOC shutdowns and to assess its potential role in deglaciations, we use a suite of long simulations conducted with a comprehensive coupled ocean-atmosphere model.

2. Methods

All simulations shown here use the coupled ocean-atmosphere model CM2Mc, as described in *Galbraith et al*. [2011]. In brief, this includes: a 3° finite volume atmospheric model, similar to that used in the Geophysical Fluid Dynamics Laboratory Earth System Model (GFDL ESM2) [*Dunne et al*., 2012]; MOM5, a non-Bousinnesq ocean model with a fully nonlinear equation of state, subgrid-scale parameterizations for mesoscale and submesoscale turbulence, vertical mixing with the K-profile parameterization scheme as well as due to the interaction of tidal waves with rough topography but otherwise a very low background vertical diffusivity (0.1 $cm^2\,s^{-1}$), similar to that used in the GFDL ESM2M model; a sea ice module, static land module, and a coupler to exchange fluxes between the components. The model does not use flux corrections but allows the ocean and atmosphere to freely achieve their steady state.

Simulations were run under "glacial" conditions, for which ice sheet albedo and surface topography were altered to Last Glacial Maximum conditions, the Bering Strait was closed, average ocean salinity was increased by 1 practical salinity unit, and atmospheric CO_2 concentration was decreased to 180 ppmv. In order to further test the robustness of the radiative effects to boundary conditions, four simulations with varying orbital configurations were conducted, in which the obliquity was set to either 22.0° or 24.5° (spanning the calculated range of the last 5 Myr), and the precessional phase, defined as the angle between the Earth's position during the Northern Hemisphere autumnal equinox and the perihelion, was set to two opposing values: 270°, at which the most severe boreal seasonal extrema occur, and 90°, at which the most severe austral seasonal extrema occur. The eccentricity was maintained at an average Quaternary value of 0.03. All simulations were initialized from an equilibrated preindustrial control state and integrated for 5000 years prior to the freshwater forcing. The AMOC is strong in all equilibrated simulations, extending to approximately 3 km depth under preindustrial conditions and to approximately 2 km depth under glacial conditions [*Brown and Galbraith*, 2015], consistent with observational inferences for a shallower AMOC during the glacial [*Thornalley et al*., 2013]. Freshwater additions were made as a "real" freshwater flux of 0.2 sverdrup, consistent with the estimated meltwater flux from the Laurentide ice sheet during HS1 [*Clement and Peterson*, 2008], applied to a rectangular region bounded by 40:60°N and 55:10°W, raising global sea level by 17 m over 1000 years.

3. Results

Freshwater input disrupts the simulated AMOC (Figure 1a) for as long as it is applied, preventing the release of heat from the subsurface Atlantic by deep convection and reducing the northward oceanic heat transport. This disruption results in a rapid cooling of the global average surface air temperature (Figure 1b) as the reduced oceanic heat transport to high northern latitudes causes the expansion of Northern Hemisphere sea ice and low-level clouds [*Herweijer et al*., 2005; *Zhang et al*., 2010] and reduces the atmospheric water vapor content [*Laurian et al*., 2009]. Although the Southern Hemisphere warms, it does so by much less than

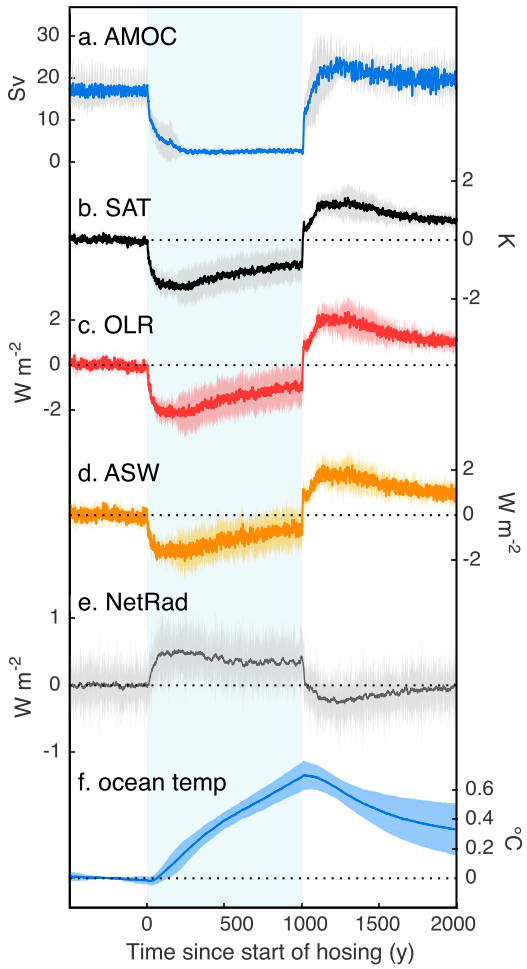

Figure 1. Ensemble of idealized water hosing experiments. Each panel shows the mean and 1 standard deviation for a four-member ensemble integrated under glacial boundary conditions. Freshwater was steadily added to the North Atlantic during years 0 to 1000 (shaded blue). All other boundary conditions were held constant throughout. (a) Atlantic Meridional Overturning at 40°N (AMOC); (b) global surface air temperature anomaly (SAT); (c) global outgoing longwave radiation anomaly (OLR); (d) global absorbed shortwave anomaly (ASW); (e) global net radiative imbalance (NetRad, mean shows 20 year boxcar filter); and (f) global ocean average temperature anomaly.

the north cools, in agreement with ice core records of relatively small temperature changes in Antarctica relative to Greenland during Dansgaard-Oeschger oscillations [*European Project for Ice Coring in Antarctica*, 2006]. The resulting higher global albedo reduces ASW, but the global atmospheric cooling causes the OLR to decrease by a greater amount (Figures 1c and 1d), such that the net radiative imbalance of the planet becomes positive (Figure 1e) [*Drijfhout*, 2015].

3.1. Radiative Feedbacks

In order to consider whether or not the positive radiative imbalance is a robust response to AMOC disruption, we can conceptualize the response of the global net radiative balance at the top of atmosphere (N_{TOA}) to any radiative perturbation, F (such as might be caused by a change in greenhouse gases or aerosols) as

$$N_{TOA} = F + \lambda T_s$$

where T_s is the deviation of the global mean surface temperature from an unperturbed state and λ represents the strength of all climate feedbacks, including clouds, water vapor, and sea ice changes. The climate feedbacks can be decomposed into a shortwave component that equals the change in ASW for a given change in surface temperature, $\lambda_{SW} = \mathrm{ASW}/T_s$, and a corresponding longwave component, $\lambda_{LW} = -\mathrm{OLR}/T_s$. A decrease of T_s will lead to a decrease of OLR, given the Stefan-Boltzmann law, so that λ_{LW} will be negative (stabilizing). If ASW also decreases under global cooling, as would be expected given an increase in surface albedo (due to more clouds, snow cover, and/or sea ice), then λ_{SW} will be positive (destabilizing). This is the case for all simulations shown here.

The total climate feedback is then $\lambda = \lambda_{LW} + \lambda_{SW}$. If the magnitude of the destabilizing, positive shortwave feedback is greater than the stabilizing, negative longwave feedback (i.e., if the ASW decreases by more than the OLR, in response to a given decrease in T_s) the total feedback would be positive, meaning that the climate system is unstable [*Liu et al.*, 2016; *Roe*, 2009]. If this were true of the Earth, any small radiative perturbation would lead to a runaway snowball or greenhouse. Given that this has clearly not been the case for at least a few hundred million years, it follows that λ_{SW} does not overwhelm the λ_{LW} throughout this time period, and therefore, the net radiative response to a cooling of the Earth surface will be a positive radiative forcing across the top of atmosphere, and vice versa.

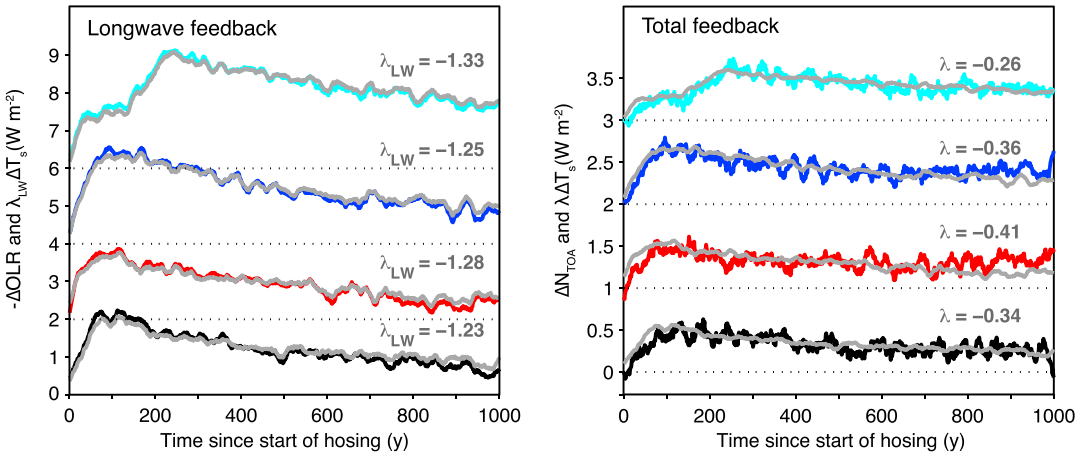

Figure 2. Radiative feedback parameters in the ensemble of glacial hosing simulations. (left) The evolution of the global mean change in OLR (colored lines) and the product of the diagnosed longwave feedback parameter and the globally averaged SAT anomaly (grey lines). (right) The equivalent quantities for N_{TOA} and the total feedback. All are 10 year running means. Black is low obliquity, weak boreal seasons; red is low obliquity, strong boreal seasons; blue is high obliquity, strong boreal seasons; and cyan is high obliquity, weak boreal seasons. The simulations are offset from each other by a constant (2 W m^{-2} for the left panel and 1 W m^{-2} for the right panel) for ease of plotting; for each simulation, zero is indicated by a dotted line. The close agreement between the colored and grey lines shows that the feedback parameters are quite stable throughout the hosing.

In our experiments, the direct energetic forcing from the imposed freshwater flux is negligible (that is, $F = 0$), but the resulting ocean and atmosphere changes excite a planetary energy imbalance via the climate feedbacks. The global mean changes in OLR and N_{TOA} over the 1000 year hosing periods in the four glacial cases were used to diagnose the feedback parameters λ and λ_{LW} (Figure 2). This was achieved simply by regressing the relevant variable (N_{TOA} and OLR, respectively) against the globally averaged surface air temperature anomaly over the hosing period. As shown, the feedback parameters are quite stable throughout the hosing and show a moderate degree of variability between the different orbital boundary conditions, with the stronger radiative imbalance (i.e., weakest λ) occurring with high obliquity and weak boreal seasons.

It is important to point out that the magnitude of the radiative imbalance will depend on the detailed response of sea ice, clouds, and ocean circulation, which cannot be perfectly reproduced by models and will therefore differ to some degree in reality. The feedbacks also vary to a large degree in space and potentially change with background climate state [*Roe et al.*, 2015; *Rose et al.*, 2014]. If changes in ocean circulation and local radiative feedbacks were to conspire so as to perfectly compensate the accumulation of heat in the subsurface North Atlantic by the removal of heat from elsewhere in the global ocean, a stable global surface air temperature could be maintained, and there would be no net radiative imbalance. However, our conceptual analysis shows that within a stable climate regime, a positive radiative imbalance is a necessary consequence of an AMOC disruption that decreases the global surface air temperature.

3.2. Planetary Warming

A positive net radiation imbalance implies heat uptake by the atmosphere, land, or ocean. If the warming were to occur largely in the atmosphere, its temperature would quickly rise, increasing the OLR to rebalance the radiation budget. Indeed, this is what climate models predict in response to a rapid increase of CO_2 above preindustrial levels, leading to restoration of radiative balance with a characteristic time scale of 200 years [*Geoffroy et al.*, 2013]. In contrast, the hosed simulations presented here are much slower to reequilibrate, displaying a climate feedback parameter λ that is ~ 1/3 of the strength shown by the same model subjected to an instantaneous doubling of CO_2. This contrast in feedbacks is reminiscent of the relatively weak feedback to natural variability, compared to anthropogenic radiative forcing, observed over the last few decades [*Xie et al.*, 2016]. These global feedback differences may, in turn, be the result of distinctive

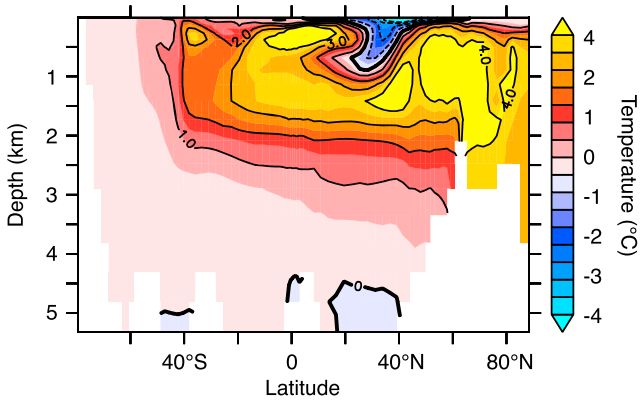

Figure 3. Change in Atlantic Ocean temperature under prolonged hosing. The change in zonally averaged temperature in the Atlantic Ocean between the last century of hosing and the prehosing state is shown for the ensemble mean (°C).

patterns of surface temperature change that occur in regions with different local radiative feedbacks [*Rose et al*., 2014]. Beyond the differences in climate feedback parameter, the slow equilibration can be conceptually rationalized in our case by the fact that the formation of North Atlantic Deep Water (NADW)—the downwelling branch of the AMOC—is a key pathway of heat exchange between the ocean and atmosphere; in its absence, the efficiency of heat exchange is substantially reduced, allowing the radiative imbalance to persist. Essentially, the disruption of oceanic heat release by deep convection in the North Atlantic allows heat to accumulate in the ocean subsurface with little expression at the ocean surface and therefore engenders a weak radiative feedback.

Our simulations show that under the radiative imbalance caused by the AMOC shutdown, the globally averaged ocean interior warms at a consistent rate of 0.07°C per century over the full 1000 years (Figure 1f). The warming is focused at 200–2000 m depth in the Atlantic ocean (Figure 3), as also occurred during HS1 in the freshwater-forced deglacial simulations of *Liu et al*. [2009] and *He et al*. [2013]. Both the magnitude of the energy imbalance and the distribution of ocean warming also agree with the model simulation shown by *Vettoretti and Peltier* [2015], in which the AMOC weakens spontaneously. Warming is focused in the middepth Atlantic because the downward mixing of heat across the low-latitude thermocline is no longer balanced by the supply of cold NADW from subpolar deep convection [*Palter et al*., 2014]. The Southern Hemisphere warming, characteristic of the bipolar seesaw, is produced by the leakage of heat from the low latitudes to outcrops in the Southern Ocean.

3.3. Potential Role of Radiative Imbalance in Deglaciation

Given that the imposed freshwater flux is a noninteractive part of the climate simulations, its effect on the energy balance can be considered an external forcing, and the magnitude of the consequent radiative imbalance can be compared to the radiative forcing of increasing CO_2. This is analogous to previous climate model estimates that compare the radiative effect of the Laurentide ice sheet and atmospheric CO_2 [*Broccoli and Manabe*, 1987]. Figure 4 shows, for the initial half of the last deglaciation, an estimate of the radiative imbalance from the AMOC disruption, compared to that implied by increasing CO_2. To calculate the forcing caused by the AMOC disruption, we take the ensemble average net radiation at the top of the atmosphere over the years 200–1000 of the glacial hosing periods and assume that the resulting value of 0.39 W m^{-2} is representative of a full AMOC shutdown. For comparison, the simulation of *Peltier and Vettoretti* [2014] showed, using the Community Earth System Model (CESM1) under glacial conditions, a radiative imbalance of 0.5 W m^{-2} between strong and weak AMOC states, suggesting that this approximate magnitude of change may be representative of comprehensive climate models. We then scale this linearly with a reconstruction of the AMOC strength (Figure 4, middle) based on radionuclide accumulation in North Atlantic sediments [*Böhm et al*., 2015; *McManus et al*., 2004], such that the full radiative effect occurs when the ^{231}Pa/^{230}Th is at its maximum. The resulting estimate (Figure 4, bottom), albeit simplistic, implies that the radiative impact of the seesaw was of comparable importance to rising CO_2 in driving planetary warming prior to 17 ka and remained at least one third as important as CO_2 until 15.3 ka, causing on the order of one third of the time-integrated radiative forcing over HS1.

The energy derived from the AMOC-induced radiative imbalance would have accumulated in the ocean interior, while surface air temperatures remained relatively low, until the start of the Bølling at approximately 14.6 ka, when the accumulated heat would have been rapidly released to the atmosphere by the resumption

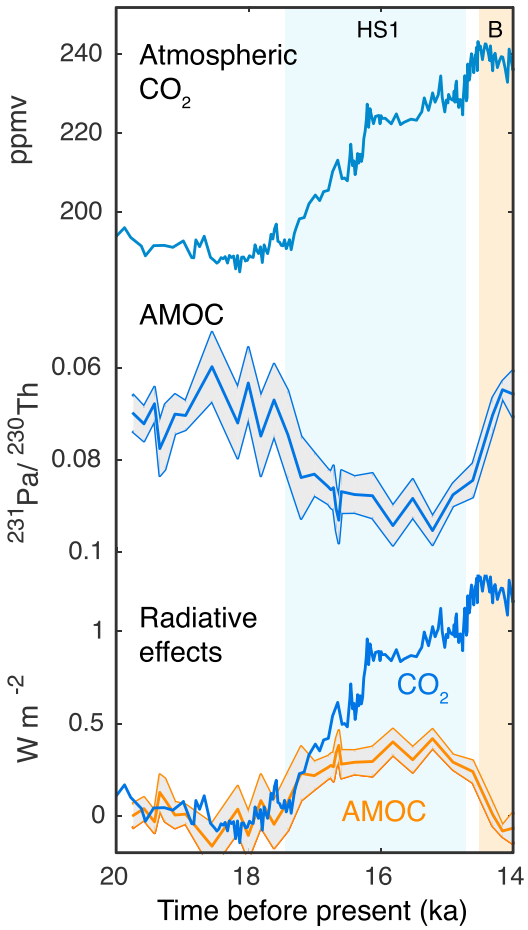

Figure 4. Contribution of the radiative effect of an AMOC disruption to the last deglaciation. The top panel shows atmospheric CO_2 reconstructed from ice core measurements over the last deglaciation. Shaded intervals highlight Heinrich Stadial 1 (HS1) and the Bølling (B). Middle panel shows the AMOC reconstructed from sedimentary radionuclide measurements at Bermuda Rise [*McManus et al*., 2004]. The bottom panel shows the radiative effect of CO_2, compared to the effect of the AMOC weakening assuming full strength during the LGM, complete shutdown during HS1, and a radiative effect equal to the ensemble mean (0.39 W m^{-2} for the full shutdown). The radiative impact of atmospheric CO_2 over the early deglaciation was estimated as $F_{CO2} = 3.6 \log_2 (CO_2/190$ ppmv), following *Myhre* et al. [1998].

of deep convection in the North Atlantic [*Liu et al*., 2009]. This scenario is similar to the "thermobaric capacitor" proposed by [*Adkins et al*., 2005], which *Thiagarajan et al*. [2014] suggested may have played a critical role in the transition of ocean circulation from a glacial to an interglacial state, but the energy is supplied by the net radiative imbalance rather than geothermal heat (which is an order of magnitude smaller). In fact, the simulated temperatures in the North Atlantic interior rise by as much as 4° C by the end of the 1000 year hosing, in the ensemble average, matching the maximum magnitude of warming during HS1 estimated by *Thiagarajan et al*. [2014] using fossil deep sea corals collected between 1000 and 2600 m depth on the New England Seamounts.

Subsequently, the release of oceanic heat over the first century following AMOC resumption produces a global surface air temperature warming of 1.4°C in the ensemble average (Figure 1), including warming at the locations of Greenland ice cores that agree closely with reconstructed warming at the Bølling transition (*simulated*, observed [*Buizert et al*., 2014]: North Greenland Eemian Ice Drilling Project *8.6*, 8.9 ± 2.4; Greenland Ice Sheet Project-2 *11.7*, 14.4 ± 1.9; and North Greenland Ice Core Project (NGRIP) *10.3*, 11.1 ± 2.8). This close agreement between model and observations suggests that the simulated accumulation of oceanic heat during the hosing experiments is similar to what actually occurred during the early deglaciation. A comparable Greenland warming was simulated by the Community Climate System Model version 3 (CCSM3) for the Bølling transition [*Buizert et al*., 2014; *He et al*., 2013; *Liu et al*., 2009], which was also attributed to the release of heat accumulated in the North Atlantic under freshwater forcing. Our experiments show that despite a subsequent gradual cooling, the simulated global surface air temperature remains 0.6°C warmer than its initial state and the ocean more than 0.3°C warmer than its initial state, even a thousand years after the AMOC resumption.

4. Discussion and Conclusions

The potential for AMOC disruptions to have destabilized glacial climates is tempered by the reconstructed evidence of Heinrich Stadial 2 (HS2). This event, which occurred between 26 and 23 ka—just 8 kyr before HS1, when the land-based ice sheet configuration was similar—appears to have been accompanied by a similar, though perhaps slightly smaller AMOC disruption [*Böhm et al*., 2015; *Gutjahr and Lippold*, 2011]. Yet

deglaciation did not occur. This is particularly notable given the presence of a well-developed Heinrich layer of ice-rafted detritus, suggesting that an ice shelf collapse occurred [*Gutjahr and Lippold*, 2011] and a pulse of warming recorded in the NGRIP ice core as a 2‰ $\delta^{18}O$ drop at the end of HS2 [*Andersen et al*., 2004], roughly half the magnitude at the start of the Bølling. Thus, either the AMOC disruption during HS2 led to significantly less heat accumulation than during HS1 (as might be expected given the lower obliquity and stronger boreal seasons at the time of HS2) or the direct impacts of an AMOC disruption (including the destabilization of floating ice shelves) are not sufficient to drive deglaciation on their own. Nonetheless, it is possible that AMOC disruption is an essential ingredient of deglaciation, in addition to factors such as the response of glaciers to precessional forcing, details of ice sheet geometry, or CO_2 release by deep convection in the Southern Ocean [*Jaccard et al*., 2016] or geological carbon [*Lund et al*., 2016].

In conclusion, our model simulations suggest that, all else being equal, the overall cooling of the Earth's surface caused by an AMOC disruption produces a positive radiative imbalance of approximately 0.4 W m^{-2}. This simulated imbalance is remarkably stable on a millennial time scale and leads to the accumulation of a large amount of heat in the ocean, focused at middepths of the North Atlantic. When released to the atmosphere by deep convection upon resumption of the AMOC, this heat leads to warmer global surface air temperatures. As such, the "bipolar temperature seesaw" was not simply a zero-sum oscillation of surface temperature between hemispheres but significantly impacted the heat content of the climate system. This mechanism would have contributed to deglaciations to some degree, though further work is required in order to determine whether or not it was a decisive factor.

Acknowledgments
We thank Nicolas Brown and Simon Yang for assistance with the model simulations and thank Graham Mortyn, Shaun Marcott, Sam Jaccard, Thomas Stocker, and Luke Skinner for discussions. Simulations were run on the Scinet facility at the University of Toronto, through a resource allocation provided by Compute Canada. Computational infrastructure was provided by the Canadian Foundation for Innovation. The CM2Mc model code is available from the Geophysical Fluid Dynamics Laboratory.

References

Adkins, J. F., A. P. Ingersoll, and C. Pasquero (2005), Rapid climate change and conditional instability of the glacial deep ocean from the thermobaric effect and geothermal heating, *Quat. Sci. Rev.*, *24*(5–6), 581–594.

Alvarez-Solas, J., S. Charbit, C. Ritz, D. Paillard, G. Ramstein, and C. Dumas (2010), Links between ocean temperature and iceberg discharge during Heinrich events, *Nat. Geosci.*, *3*(2), 122–126, doi:10.1038/ngeo752.

Alvarez-Solas, J., M. Montoya, C. Ritz, G. Ramstein, S. Charbit, C. Dumas, K. Nisancioglu, T. Dokken, and A. Ganopolski (2011), Heinrich event 1: An example of dynamical ice-sheet reaction to oceanic changes, *Clim. Past*, *7*, 1297–1306.

Andersen, K. K., et al. (2004), High-resolution record of Northern Hemisphere climate extending into the last interglacial period, *Nature*, *431*(7005), 147–151.

Anderson, R. F., S. Ali, L. I. Bradtmiller, S. H. H. Nielsen, M. Q. Fleisher, B. E. Anderson, and L. H. Burckle (2009), Wind-driven upwelling in the Southern Ocean and the deglacial rise in atmospheric CO_2, *Science*, *323*(5920), 1443–1448, doi:10.1126/Science.1167441.

Barker, S., P. Diz, M. J. Vautravers, J. Pike, G. Knorr, I. R. Hall, and W. S. Broecker (2009), Interhemispheric Atlantic seesaw response during the last deglaciation, *Nature*, *457*(7233), 1097–U1050, doi:10.1038/Nature07770.

Barker, S., G. Knorr, R. L. Edwards, F. Parrenin, A. E. Putnam, L. C. Skinner, E. Wolff, and M. Ziegler (2011), 800,000 years of abrupt climate variability, *Science*, *334*(6054), 347–351, doi:10.1126/Science.1203580.

Böhm, E., J. Lippold, M. Gutjahr, M. Frank, P. Blaser, B. Antz, J. Fohlmeister, N. Frank, M. Andersen, and M. Deininger (2015), Strong and deep Atlantic Meridional Overturning Circulation during the last glacial cycle, *Nature*, *517*(7532), 73–76.

Broccoli, A., and S. Manabe (1987), The influence of continental ice, atmospheric CO_2, and land albedo on the climate of the last glacial maximum, *Clim. Dyn.*, *1*(2), 87–99.

Broecker, W. S. (1998), Paleocean circulation during the last deglaciation: A bipolar seesaw?, *Paleoceanography*, *13*(2), 119–121, doi:10.1029/97PA03707.

Brown, N., and E. Galbraith (2015), Hosed vs. unhosed: Global response to interruptions of the Atlantic Meridional Overturning, with and without freshwater forcing, *Clim. Past Discuss.*, *11*, 4669–4700.

Buizert, C., et al. (2014), Greenland temperature response to climate forcing during the last deglaciation, *Science*, *345*(6201), 1177–1180, doi:10.1126/science.1254961.

Cheng, H., R. L. Edwards, W. S. Broecker, G. H. Denton, X. G. Kong, Y. J. Wang, R. Zhang, and X. F. Wang (2009), Ice age terminations, *Science*, *326*(5950), 248–252, doi:10.1126/Science.1177840.

Clement, A. C., and L. C. Peterson (2008), Mechanisms of abrupt climate change of the last glacial period, *Rev. Geophys.*, *46*, RG4002, doi:10.1029/2006RG000204.

Crowley, T. J. (1992), North Atlantic deep water cools the Southern Hemisphere, *Paleoceanography*, *7*(4), 489–497, doi:10.1029/92PA01058.

Dokken, T. M., K. H. Nisancioglu, C. Li, D. S. Battisti, and C. Kissel (2013), Dansgaard-Oeschger cycles: Interactions between ocean and sea ice intrinsic to the Nordic seas, *Paleoceanography*, *28*, 491–502, doi:10.1002/palo.20042.

Drijfhout, S. S. (2015), Global radiative adjustment after a collapse of the Atlantic Meridional Overturning Circulation, *Clim. Dyn.*, *45*(7–8), 1789–1799.

Dunne, J. P., et al. (2012), GFDL's ESM2 Global Coupled Climate–Carbon Earth System Models. Part I: Physical formulation and baseline simulation characteristics, *J. Clim.*, *25*(19), 6646–6665, doi:10.1175/jcli-d-11-00560.1.

European Project for Ice Coring in Antarctica, c. m (2006), One-to-one coupling of glacial climate variability in Greenland and Antarctica, *Nature*, *444*, 195–198.

Galbraith, E. D., et al. (2011), Climate variability and radiocarbon in the CM2Mc Earth System Model, *J. Clim.*, *24*(16), 4230–4254, doi:10.1175/2011JCLi3919.1.

Geoffroy, O., D. Saint-Martin, D. J. Olivié, A. Voldoire, G. Bellon, and S. Tytéca (2013), Transient climate response in a two-layer energy-balance model. Part I: Analytical solution and parameter calibration using CMIP5 AOGCM experiments, *J. Clim.*, *26*(6), 1841–1857.

Gutjahr, M., and J. Lippold (2011), Early arrival of Southern Source Water in the deep North Atlantic prior to Heinrich event 2, *Paleoceanography*, *26*, PA2101, doi:10.1029/2011PA002114.
He, F., J. D. Shakun, P. U. Clark, A. E. Carlson, Z. Liu, B. L. Otto-Bliesner, and J. E. Kutzbach (2013), Northern Hemisphere forcing of Southern Hemisphere climate during the last deglaciation, *Nature*, *494*(7435), 81–85.
Herweijer, C., R. Seager, M. Winton, and A. Clement (2005), Why ocean heat transport warms the global mean climate, *Tellus A*, *57*(4), 662–675.
Jaccard, S. L., E. D. Galbraith, A. Martínez-García, and R. F. Anderson (2016), Covariation of deep Southern Ocean oxygenation and atmospheric CO_2 through the last ice age, *Nature*, *530*(7589), 207–210.
Köhler, P., H. Fischer, G. Munhoven, and R. E. Zeebe (2005), Quantitative interpretation of atmospheric carbon records over the last glacial termination, *Global Biogeochem. Cycles*, *19*, GB4020, doi:10.1029/2004GB002345.
Laurian, A., S. Drijfhout, W. Hazeleger, and R. van Dorland (2009), Global surface cooling: The atmospheric fast feedback response to a collapse of the thermohaline circulation, *Geophys. Res. Lett.*, *36*, L20708, doi:10.1029/2009GL040938.
Lee, S. Y., J. C. H. Chiang, K. Matsumoto, and K. S. Tokos (2011), Southern Ocean wind response to North Atlantic cooling and the rise in atmospheric CO_2: Modeling perspective and paleoceanographic implications, *Paleoceanography*, *26*, PA1214, doi:10.1029/2010PA002004.
Liu, Z., et al. (2009), Transient simulation of last deglaciation with a new mechanism for Bolling-Allerod warming, *Science*, *325*(5938), 310–314, doi:10.1126/science.1171041.
Liu, Z., H. Yang, C. He, and Y. Zhao (2016), A theory for Bjerknes compensation: The role of climate feedback, *J. Clim.*, *29*(1), 191–208.
Lund, D., P. Asimow, K. Farley, T. Rooney, E. Seeley, E. Jackson, and Z. Durham (2016), Enhanced East Pacific Rise hydrothermal activity during the last two glacial terminations, *Science*, *351*(6272), 478–482.
Marcott, S. A., P. U. Clark, L. Padman, G. P. Klinkhammer, S. R. Springer, Z. Liu, B. L. Otto-Bliesner, A. E. Carlson, A. Ungerer, and J. Padman (2011), Ice-shelf collapse from subsurface warming as a trigger for Heinrich events, *Proc. Natl. Acad. Sci. U.S.A.*, *108*(33), 13,415–13,419.
McManus, J. F., D. W. Oppo, and J. L. Cullen (1999), A 0.5-million-year record of millennial-scale climate variability in the North Atlantic, *Science*, *283*(5404), 971–975.
McManus, J. F., R. Francois, J. M. Gherardi, L. D. Keigwin, and S. Brown-Leger (2004), Collapse and rapid resumption of Atlantic meridional circulation linked to deglacial climate changes, *Nature*, *428*(6985), 834–837.
Menviel, L., M. England, K. Meissner, A. Mouchet, and J. Yu (2014), Atlantic-Pacific seesaw and its role in outgassing CO_2 during Heinrich events, *Paleoceanography*, *29*, 58–70, doi:10.1002/2013PA002542.
Myhre, G. B., E. J. Highwood, K. P. Shine, and F. Stordal (1998), New estimates of radiative forcing due to well mixed greenhouse gases, *Geophys. Res. Lett.*, *25*(14), 2715–2718.
Palter, J. B., S. M. Griffies, B. L. Samuels, E. D. Galbraith, A. Gnanadesikan, and A. Klocker (2014), The deep ocean buoyancy budget and its temporal variability, *J. Clim.*, *27*(2), 551–573.
Peltier, W. R., and G. Vettoretti (2014), Dansgaard-Oeschger oscillations predicted in a comprehensive model of glacial climate: A "kicked" salt oscillator in the Atlantic, *Geophys. Res. Lett.*, *41*, 7306–7313, doi:10.1002/2014GL061413.
Roe, G. (2009), Feedbacks, timescales, and seeing red, *Annu. Rev. Earth Planet. Sci.*, *37*, 93–115.
Roe, G. H., N. Feldl, K. C. Armour, Y.-T. Hwang, and D. M. Frierson (2015), The remote impacts of climate feedbacks on regional climate predictability, *Nat. Geosci.*, *8*(2), 135–139.
Rose, B. E., K. C. Armour, D. S. Battisti, N. Feldl, and D. D. Koll (2014), The dependence of transient climate sensitivity and radiative feedbacks on the spatial pattern of ocean heat uptake, *Geophys. Res. Lett.*, *41*, 1071–1078, doi:10.1002/2013GL058955.
Schmittner, A., and E. D. Galbraith (2008), Glacial greenhouse-gas fluctuations controlled by ocean circulation changes, *Nature*, *456*(7220), 373–376, doi:10.1038/nature07531.
Stocker, T. F., and S. J. Johnsen (2003), A minimum thermodynamic model for the bipolar seesaw, *Paleoceanography*, *18*(4), 1087, doi:10.1029/2003PA000920.
Thiagarajan, N., A. V. Subhas, J. R. Southon, J. M. Eiler, and J. F. Adkins (2014), Abrupt pre-Bolling-Allerod warming and circulation changes in the deep ocean, *Nature*, *511*(7507), 75–78, doi:10.1038/nature13472.
Thornalley, D. J., S. Barker, J. Becker, I. R. Hall, and G. Knorr (2013), Abrupt changes in deep Atlantic circulation during the transition to full glacial conditions, *Paleoceanography*, *28*, 253–262, doi:10.1002/palo.20025.
Toggweiler, J., and D. W. Lea (2010), Temperature differences between the hemispheres and ice age climate variability, *Paleoceanography*, *25*, PA2212, doi:10.1029/2009PA001758.
Vellinga, M., R. A. Wood, and J. M. Gregory (2002), Processes governing the recovery of a perturbed thermohaline circulation in HadCM3, *J. Clim.*, *15*(7), 764–780.
Vettoretti, G., and W. R. Peltier (2015), Interhemispheric air temperature phase relationships in the nonlinear Dansgaard-Oeschger oscillation, *Geophys. Res. Lett.*, *42*, 1180–1189, doi:10.1002/2014GL062898.
Xie, S.-P., Y. Kosaka, and Y. M. Okumura (2016), Distinct energy budgets for anthropogenic and natural changes during global warming hiatus, *Nat. Geosci.*, *9*(1), 29–33.
Zhang, R., S. M. Kang, and I. M. Held (2010), Sensitivity of climate change induced by the weakening of the Atlantic Meridional Overturning Circulation to cloud feedback, *J. Clim.*, *23*(2), 378–389.